Diversity of murtoos and murtoo-related subglacial landforms in the Finnish area of the Fennoscandian Ice Sheet

ANTTI E. K. OJALA (iD), JONI MÄKINEN, ELINA AHOKANGAS, KARI KAJUUTTI, MARKUS VALKAMA, ALEKSI TUUNAINEN AND JUKKA-PEKKA PALMU

BOREAS

Murtoos are recently discovered triangular-shaped subglacial landforms that form under warm-based ice and in association with significant subglacial meltwater flow. They appear in distinct fields and commonly occur in the area that was covered by the Fennoscandian Ice Sheet during glacial periods. Murtoos potentially represent a transition form from non-channelized to channelized subglacial drainage networks. In the present study, we analyse and classify murtoos and murtoo-related landforms in the Finnish area of the Fennoscandian Ice Sheet based on their characteristics and appearance in LiDAR-based digital elevations models. Combined with morphometric analyses, the observations suggest that five types of murtoos and murtoo-related landforms are common and widespread in Finland: (i) triangle-type murtoos (TTMs), (ii) chevron-type murtoos (CTMs), (iii) lobate-type murtoos (LTMs), (iv) murtoo-related ridges and escarpments (MREs), and (v) other murtoo-related polymorphous landforms (PMRs) that look like small mounds and ridges. The morphometric characteristics of the different types are described here in detail, and it is shown that they are spatially and geomorphologically related. In addition, we provide examples of murtoos other than the TTMs to demonstrate that different murtoo types and murtoo-related landforms are composed of similar sediments and architectural characteristics. The diversity of murtoo landforms and the transition between distinct murtoo types indicate rapid and complicated variations in the configuration of subglacial hydrology at different spatial and temporal scales. This study emphasizes the essential role of subglacial meltwater in the shaping of glacial landscapes and the redistribution of large volumes of sediments during the deglaciation of the Fennoscandian Ice Sheet.

Antti E. K. Ojala (antti.ojala@gtk.fi), Geological Survey of Finland, P.O. Box 96, Espoo FI-02151, Finland and Department of Geography and Geology, University of Turku, Turku FI-20014, Finland; Markus Valkama, Aleksi Tuunainen and Jukka-Pekka Palmu, Geological Survey of Finland, P.O. Box 96, FI-02151 Espoo, Finland; Joni Mäkinen, Elina Ahokangas and Kari Kajuutti, Department of Geography and Geology, University of Turku, FI-20014 Turku, Finland;

Mäkinen *et al.* (2017), Peterson *et al.* (2017) and Ojala *et al.* (2019a) recently described a new morphologically distinct triangular-shaped subglacial landform in Finland and Sweden, which was subsequently called a 'murtoo'. In the present paper, these triangular-shaped murtoos are hereafter referred to as triangle-type murtoos (TTMs). The morphometric and sedimentological characteristics, as well as the spatial distribution of TTMs in the Fennoscandian Ice Sheet (FIS) area indicate that they were formed under warm-based ice and in association with significant subglacial meltwater flow during rapid deglaciation in a warming climate (Mäkinen *et al.* 2019; Ojala *et al.* 2019a). Murtoos are important, because they can constrain the behaviour of past ice sheets and glaciers.

Recent studies on glacial hydrology have demonstrated that meltwater supply and drainage, as well as the distribution of hydrological networks beneath the ice sheets, are among the main determinants of ice-flow variations over different time scales, with hydraulic capacity and subglacial water pressure playing significant roles (e.g. Remy & Legresy 2004; Schoof 2010; Andrews *et al.* 2014; Dow *et al.* 2015; Flowers, 2015; Rada & Schoof 2018; Davison *et al.* 2019). The conditions underneath ice sheets, such as terrain topography,

bedrock permeability and the spatial distribution of glacial sediments, connected with subglacial groundwater flow, are also an integral part of glaciological systems (e.g. Bell *et al.* 2007; Siegert *et al.* 2017; Hermanowski & Piotrowski 2019). Moreover, subglacial processes and hydrological networks, including the distribution and drainage of subglacial lakes, can substantially contribute to sediment distribution underneath active ice lobes (Benn & Evans 1998; Lesemann *et al.* 2014; Bowling *et al.* 2019; Davison *et al.* 2019).

While eskers have long been recognized as channelized drainage networks under former ice sheets (Shreve 1972), landforms and sedimentary processes in non-channelized environments have remained less well understood (e.g. Shaw *et al.* 1989, 2008; Boulton *et al.* 2001; Möller & Dowling 2018). In fact, sedimentary elements formed at the transition between inefficient distributed (sheets and films, cavities) and efficient (channelized) subglacial drainage environments (e.g. Flowers, 2015) over crystalline bedrock are poorly disentangled. Based on trench excavations, TTMs are found to be composed of clay-poor diamictons that were produced by sediment-concentrated creep and some sorting in a non-channelized subglacial environment under effective pressure close to zero (Mäkinen

et al. 2017, 2019). In Finland, the distribution of murtoos is associated with the active ice lobes of the FIS (Boulton *et al.* 2001), and they often occur along subglacial meltwater corridors that are sometimes transitional to eskers (Mäkinen *et al.* 2017; Ojala *et al.* 2019a) (Fig. 1). It has been hypothesized that murtoos represent a transition from non-channelized to channelized meltwater drainage networks, and thereby offer high potential to improve our understanding of

subglacial hydrology and the related modelling of rapidly melting ice sheets (Mäkinen *et al.* 2017, 2019).

The first ice sheet-scale mapping of murtoos in Sweden and Finland was conducted by Ojala *et al.* (2019a). Using LiDAR-based digital elevation models (DEMs), they registered murtoo fields that were distinguished as a 'field' if they contained at least five distinct TTMs. Altogether, they identified 149 and 410 murtoo fields in Finland and Sweden, respectively (Fig. 1). Consistently
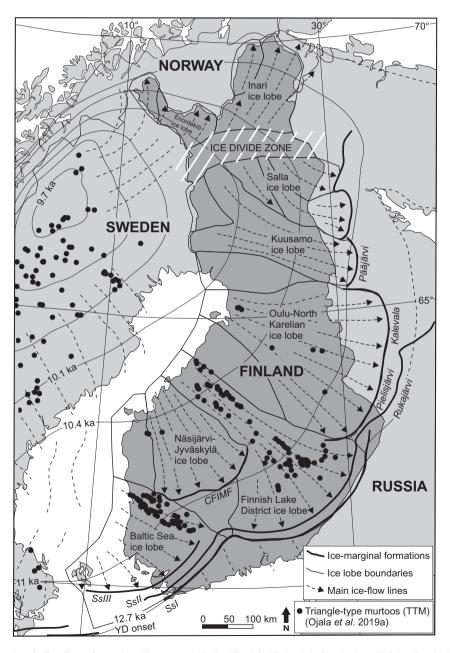

Fig. 1. The ice lobes and main flowlines of postulated ice streams (dashed lines) in Finland during the Late Weichselian deglaciation (after Rainio *et al.* 1995; Kleman *et al.* 1997; Boulton *et al.* 2001; Greenwood *et al.* 2017; Putkinen *et al.* 2017). The ice-marginal formations (SsI–SsIII = Salpausselkäs; CFIMF = Central Finland ice-marginal formation) are indicated with thicker black lines, the selected FIS retreat isochrones with thinner black lines (Hughes *et al.* 2015), and fields of triangle-type murtoos (Ojala *et al.* 2019a) with black dots.

with Mäkinen *et al.* (2017), Ojala *et al.* (2019a) noticed that an abundance of landforms that are very similar to TTMs occurs alongside them, with sharp edges, a clear orientation and an asymmetric profile. However, Ojala *et al.* (2019a) excluded these from their murtoo inventory, because these landforms did not exhibit a clear and diagnostic triangular shape. Based on this observation, they even suggested that a suitable subglacial environment and circumstances in which murtoos were formed may have been more widespread in the FIS area during deglaciation than their mapped TTM fields indicate.

In this paper, the morphological inventory and analysis of murtoos in the Finnish area of the FIS are expanded. First, the inventory of murtoos by Ojala *et al.* (2019a) in Finland is revisited and extended to cover landforms that are spatially associated with and geomorphologically similar to TTMs. Second, the predominant morphometric characteristics of different murtoo types and murtoo-related landforms are established and compared with the data earlier presented by Ojala *et al.* (2019a) for TTMs. Finally, an updated spatial data set of murtoos in Finland is presented. Our approach is based on the morphometric, spatial and geomorphic relationships between TTMs (Ojala *et al.* 2019a) and other murtoo types, as well as their subsurface sedimentary characteristics established by means of trench excavations at selected locations. The present results are expected to increase understanding of the variety of murtoos and murtoo-related landforms in the FIS area, as well as subglacial (meltwater) processes.

Study area

The study area in Finland has been several times subjected to erosional and depositional activities during the late Quaternary glaciations (Hughes *et al.* 2020). During the Weichselian maximum ice coverage event, around 23–19 ka BP, Finland was completely covered by the Fennoscandian Ice Sheet (FIS), and the southern margin of the FIS extended far south into continental Europe (e.g. Hughes *et al.* 2015). By around 13 ka BP, during deglaciation, the ice margin had retreated to southern coastal Finland (e.g. Hughes *et al.* 2015). Soon after, during the Younger Dryas period (*c*. 12.8–11.7 ka BP; Alley *et al.* 2003), the ice-sheet margin remained stationary or re-advanced as a result of climate cooling and formed the most conspicuous glacial formations in Fennoscandia, known as the Salpausselkä ice-marginal formations in Finland (e.g. Rainio *et al.* 1995) (Fig. 1). The Younger Dryas ice-marginal formations can be traced through the Scandinavian Peninsula, southern Finland, Russian Karelia and the Kola Peninsula (e.g. Donner 1995). At that time, the FIS was divided into several active ice lobes, bordered by each other or by more passive areas, which operated time-transgressively (Punkari 1980; Kleman *et al.* 1997; Boulton *et al.* 2001; Fig. 1). The reason for this separation and highly

complex behaviour of the ice lobes was related to terrain topography and regional differences in the accumulation of ice (Punkari 1980), but the role of subglacial hydrology and flooding beneath the FIS has remained less well explored, even though subglacial drainage has been proven to initiate and maintain the rapid flow of modern ice sheets (e.g. Bell *et al.* 2007; Flowers, 2015).

The Early Holocene climate warming initiated rapid melting and continuous retreat of the ice sheet north of the Salpausselkä ice-marginal positions. The Central Finland ice-marginal formation (CFIMF) was formed around 11 ka BP and has been considered to represent a re-advance of the Näsijärvi–Jyväskylä ice lobe (Rainio 1996; Fig. 1). The final deglaciation of the FIS progressed rapidly, and the entire ice sheet was gone by 9–10 ka BP (Hughes *et al.* 2015).

The crystalline Precambrian bedrock of the Fennoscandian Shield is covered by glacial and interglacial sediments, most of which have been stripped away or at least deformed by the subsequent glaciations (Rainio *et al.* 1995; Lehtinen *et al.* 2005). The Salpausselkäs and other large ice-marginal formations in Fennoscandia are important landforms for glacial dynamic considerations, as they indicate the terminus of the active ice lobes during the Late Weichselian/Early Holocene deglaciation (Fig. 1). They are composed of terminal moraine ridges, ice-contact fans, sandurs and glaciofluvial deltas, with a diverse spatial appearance (Rainio *et al.* 1995). The more levelled ground in Finland is covered by Weichselian till and ice-flow-parallel lineations, such as drumlins and fluted till, which occur over most of the Scandinavian Shield area (Lundqvist & Saarnisto 1995; Kleman *et al.* 1997). The lineations indicate that the glacier was warm-based during the Late Weichselian (e.g. Benn & Evans 1998; Möller & Dowling 2018). A wide variety of ice-flow transverse moraine ridges and undirected landforms are also present, such as De Geer moraine (Ojala 2016), ribbed moraine areas (Kurimo 1980; Sarala 2006) and different types of hummocky moraine areas (e.g. Lundqvist & Saarnisto 1995; Putkinen *et al.* 2017). Tracts of hummock corridors, which stand out from the streamlined drumlinized bed, often exhibit elongated shapes in relation to the ice-flow direction and have been interpreted as formed by subglacial meltwater pathways in the FIS area (Peterson & Johnson 2018; Lewington *et al.* 2019). Moreover, Ojala *et al.* (2019a) noticed that murtoo fields, which are mostly found in the areas of the Finnish Lake District, Baltic Sea and Oulu–North Karelian ice lobes in southern and central Finland, have often been mapped as 'dead-ice' hummocky moraines in traditional Quaternary mapping prior to the availability of high-resolution LiDAR-based digital elevation models (DEMs; Fig. 1).

The boundary zones of active ice lobes are often characterized by large eskers and/or glaciofluvial interlobate complexes (Punkari 1980; Lundqvist & Saarnisto 1995). Eskers, either as single longitudinal ridges

or in more complex glacifluvial landform assemblages, also occur within ice lobe areas, aligned parallel to the regional ice flow. They were formed in subglacial tunnels and open crevasses close to the ice margin (Shreve 1972; Benn & Evans 1998). Shackleton *et al.* (2018) reconstructed the temporal and spatial evolution of subglacial drainage beneath the FIS. They demonstrated the abundance of potential subglacial lakes and drainage pathways beneath the FIS during the Late Weichselian deglaciation (22–10 ka BP) and suggested that ice-sheet dynamics were affected by the fill and drain cycles of subglacial lakes in the onset zones and at the margins of ice streams. More recently, Ahokangas *et al.* (2020) initiated the mapping and classification of drainage routes in the Finnish area of the FIS in association with murtoo fields.

Material and methods

Mapping and screening of murtoos and murtoo-related landforms in the present study were based on processed LiDAR DEMs (2-m resolution and vertical accuracy of 0.1–0.3 m) at the scale of 1:5000 to 1:15 000 and the LiDAR imagery-based nationwide Glacier Dynamic database (GDdatabase) of glacial landforms (Putkinen *et al.* 2017). We used several DEM visualizations, mainly of a multidirectional oblique-weighted hillshade (MDOW) (Jenness 2013) and slope derivatives (e.g. Palmu *et al.* 2015; Putkinen *et al.* 2017). The landform classes of the GDdatabase range from glacifluvial (esker, sandur, delta) to till-dominated landforms, such as De Geer and hummocky moraines, and are available via the Hakku spatial data service (https://hakku.gtk.fi/en) and the Maankamara map service (https://gtkdata.gtk.fi/maankamara). During the present screening, fields of murtoos and murtoo-related landforms were primarily delineated from combinations of DEMs and MDOWs and separated in a separate database as polygon features prior to their classification.

Since murtoos are a rather recently discovered landform, there are no previous formal or published classifications of murtoo morphology or variations in their morphology that could represent different types of murtoos. Here, we undertook a straightforward approach to classify murtoo types as well as landforms that bear certain similarities to murtoos in the ArcMap (®ESRI) environment using LiDAR remote sensing data, particularly their planform characteristics. No automated statistical algorithms or object-based image analysis were applied to enhance visual interpretation. The classification was based on experiences gained during the previous murtoo investigations in the FIS area (Mäkinen *et al.* 2017; Peterson *et al.* 2017; Ojala *et al.* 2019a), the presently conducted screening of murtoo fields in Finland and cross-sectional profiles drawn longitudinally and transversely across these landforms. The main distinctions in their morphology

(dimensions, shape and association with other landforms) were determined, and their subdivision and naming as commonly occurring types were justified based on diagnostic features.

The scheme of classification was followed by a morphometric analysis of murtoo types and murtoo-related landforms to provide quantitative insights regarding the variation in their dimensions and typical ranges within which they exist. In order to collect results that would be comparable between TTMs (Ojala *et al.* 2019a) and other murtoo types, the morphometric analyses were implemented in a similar way to Ojala *et al.* (2019a) (Fig. 2). Accordingly, width, length, height and different slope measurements were carried out in the ArcMap (®ESRI) environment based on LiDAR DEMs with details of measured features and calculated values given in Fig. 2. Measurements were taken from 100 randomly selected landforms of each type, distributed around Finland.

As remote sensing with LiDAR DEM is purely geomorphic, the present work is supplemented with studies on the subsurface sediment characteristics of landforms other than the TTMs. The presently studied sites are murtoo-related ridges in Kullaa and Kämmäkkä, an escarpment south of Mikkeli, and the limb of a chevron-type murtoo north of Mikkeli (see Results for different types). In addition to geomorphology, their characterization is based on excavations of trenches across these landforms. The main sedimentary structures and material properties are compared with TTMs (Mäkinen *et al.* 2017, 2019). Trenches (10–40 m long and 4–5 m wide) were excavated through the landforms, which were 50–100 m long, about 15–20 m wide and 2–6 m high. Vertical sections of the excavations were photographed and logged for sediment lithology and structures. Here, however, we only present and compare the main characteristics, material properties and morphological relationships between murtoo-related landforms and TTMs, while more detailed papers on their sediment structures, grain sizes and macro-fabric properties will follow.

Results

Classification of murtoos and murtoo-related landforms

In the Finnish area of the FIS, the following types and characteristics of landforms are common and widespread in murtoo fields: (i) triangle-type murtoos (TTMs; see Ojala *et al.* 2019a), (ii) chevron-type murtoos (CTMs), (iii) lobate-type murtoos (LTMs), (iv) murtoo-related ridges and escarpments (MREs) and (v) other murtoo-related polymorphous landforms (PMRs) that typically look like small mounds and ridges (Fig. 3). We stress that types i–iv are representative examples of murtoos and murtoo-related landforms but in reality, murtoo fields often contain landforms that represent
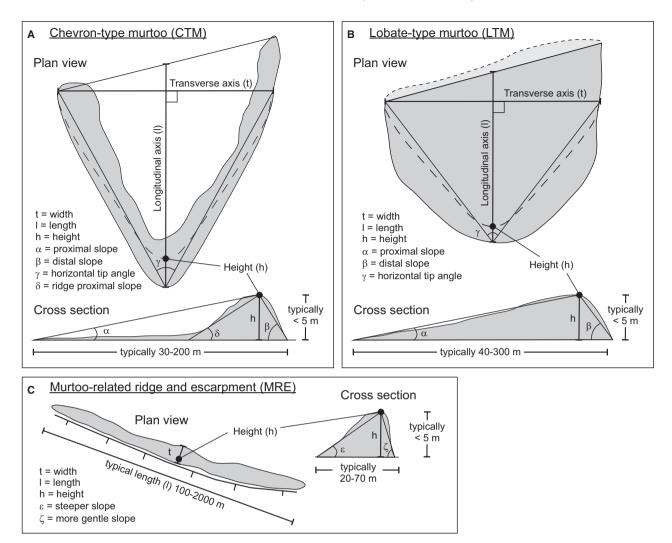
Fig. 2. Measured features and calculated values of (A) chevron-type murtoos (CTMs) and (B) lobate-type murtoos (LTMs) in the present study. The transverse (t) and longitudinal (l) axes, height (h), proximal (α) and distal (β) slopes, and horizontal tip angle (γ) are equivalent to measurements by Ojala _et al._ (2019a) conducted on triangle-type murtoos (TTMs), whereas the ridge proximal slope (δ) is an addition to that (C). For murtoo-related ridges and escarpments (MREs), the measured angles indicate steeper (ζ) and more gentle (ε) slopes along their width (t) and transverse to the longitudinal axis that represents their length (l).

transitional forms between these main classes, contain combined characteristics of different classes, or are more polymorphous landforms and thus belong to type category v.

Triangle-type murtoos (TTMs) (Fig. 3A, F) are those already described in detail by Ojala _et al._ (2019a). These landforms have the following characteristics:

- Their distinct and diagnostic feature is a triangular shape with a horizontal tip angle (γ) pointing towards the latest ice-flow direction, as was first noticed by Mäkinen _et al._ (2017).
- The longitudinal profile along the axis is asymmetric, with the distal slope (β) steeper than the proximal slope (α), and the outer edges of these landforms are straight and sharp and thereby often well defined.

- Individual TTMs are typically equally long and wide, but more elongated (or wider) forms may in some cases appear.
- The limbs of the V-shape outer edges are sometimes visible, but usually the interior of the murtoo (the core) is completely filled with glacial sediments (Mäkinen _et al._ 2017, 2019).
- Murtoo fields that are composed of TTMs sometimes exhibit a shingled appearance when partly overlapping landforms are numerous. In such cases, they often side-lap each other and form interlocking features.
- Fields of TTMs sometimes exhibit fan-shaped hollows that are part of the landform and erosional continuity (Fig. 3E).
- Especially for larger TTMs, the surfaces are frequently characterized by small ridges, hollows or other irregular patterns.
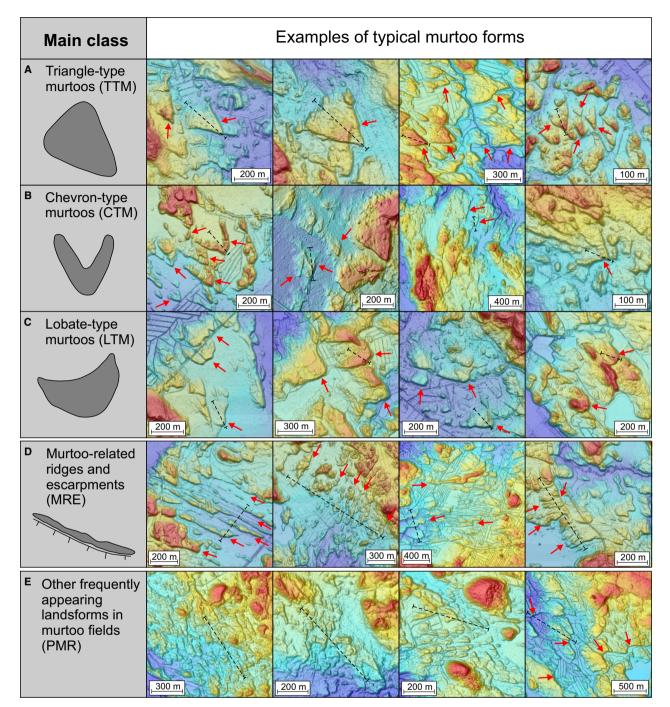
Main class	Examples of typical murtoo forms
A Triangle-type murtoos (TTM)	
B Chevron-type murtoos (CTM)	
C Lobate-type murtoos (LTM)	
D Murtoo-related ridges and escarpments (MRE)	
E Other frequently appearing landsforms in murtoo fields (PMR)	

Fig. 3. Classification and LiDAR DEM characteristics of different murtoo types and murtoo-related landforms in the Fennoscandian Ice Sheet area in Finland. Panels A–E are hillshaded LiDAR DEM examples and panels F–J their mapped interpretations. Local ice-flow directions are indicated with black arrows, red arrows on LiDAR DEMs point to typical landforms presented in each case, and dotted lines indicate the locations of elevation profiles. The locations of these examples are given in Fig. 4.

The diagnostic characteristics of chevron-type murtoos (CTMs; Fig. 3B, G) are the following:

- The V-shape ridge-type limbs of murtoos are well established while the interior lacks filling by glacial sediments.

- The tip angle (γ) points towards the latest ice-flow direction, in accordance with TTMs.
- The delimiting ridge with two limbs may form a complete chevron, or one of the limbs may be shorter ('incomplete chevron') or almost entirely missing ('half-chevron').
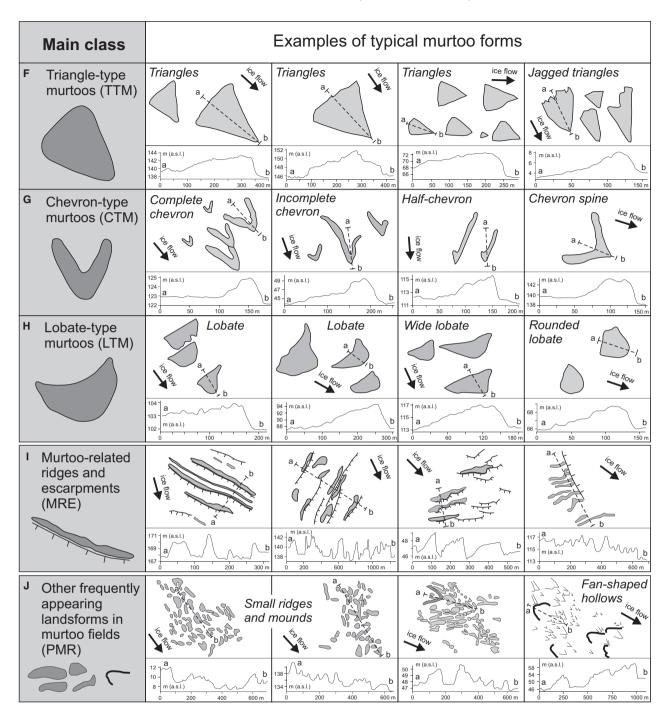
Fig. 3. (continued)

- The thickness and height of the delimiting ridge limbs may vary within a single landform.
- Uniformly with the TTMs, CTMs are often equally long and wide in the case of complete V-forms.
- The proximal slope (δ) of the ridge at the chevron tip is in most cases less steep than the distal slope (β).

The diagnostic characteristics of LTMs (Fig. 3C, H) are the following:

- The distal ending of the LTM is rounded or manifold in character and missing a horizontal sharpness of the tip angle (γ).
- The proximal part often has a concave outline and the landform direction generally points towards the latest ice-flow direction, similarly to TTMs and CTMs.
- The longitudinal axis profile of LTMs is asymmetric, with the distal slope (β) significantly steeper than the proximal slope (α).
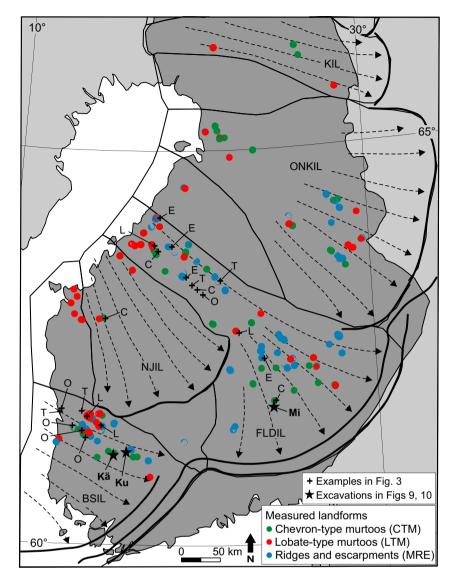
Fig. 4. Distribution of murtoo and murtoo-related ridge and escarpment examples presented in Fig. 3 (black crosses, T = triangle-type murtoos; C = chevron-type murtoos; L = lobate-type murtoos; E = murtoo-related ridges and escarpments; O = other murtoo-related polymorphous landforms) and locations of the lobate- and chevron-type murtoos and murtoo-related ridges and escarpments that were measured in the present study to produce a data set of their dimensions. The excavated sites in southern and northern Mikkeli (Mi), Kullaa (Ku) and Kämmäkkä (Kä) are identified with black stars. See Fig. 1 for abbreviations and references to the ice lobes (solid lines), the main ice-flow patterns (dashed lines) and the ice-marginal formations (thicker solid lines) in Finland.

- The edges of the landform are smooth and rounded, but steep towards the down-ice direction.
- The width and proximal shape of LTMs vary considerably.
- The outer edges of LTMs are in some cases visible, when apparent they also lack a sharp and clear tip angle (γ).

Mäkinen *et al.* (2017) already noticed that murtoos are frequently associated with distinct diagonal or slightly curved low-relief escarpments that are up to a few kilometres long and interpreted as erosional in origin. In the present study, we noticed

that these landforms are not only escarpments, but also long ridges with variable angles on their transverse slopes. The diagnostic features of murtoo-related ridges and escarpments (MREs; Fig. 3D, I) are the following:

- Depending on the overall topography and underlying bedrock structures, MREs are diagonal or slightly curved in appearance.
- They are long landforms that extend from a few hundreds of metres up to several kilometres.
- It is typical that adjacent ridges and escarpments are separated by channel-like passages or local
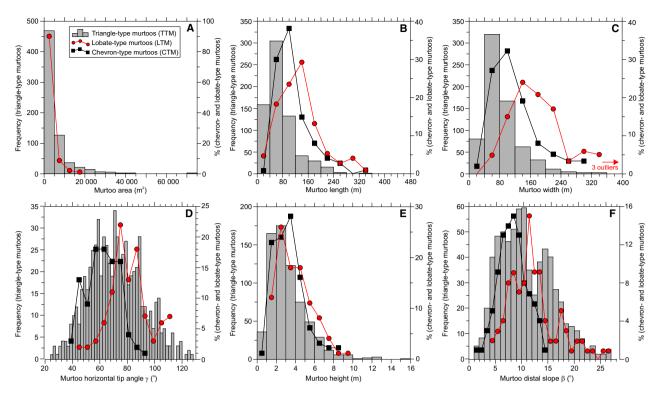
Fig. 5. Dimension variability and horizontal tip (γ) and distal slope (β) angles of the presently studied lobate-type (LTMs) and chevron-type murtoos (CTMs). Grey bars display data on the dimensions and angles of the triangle-type murtoos (TTMs) based on Ojala *et al.* (2019a).

meltwater routes that sometimes exhibit erosional characteristics.

- The distance between adjacent ridges and escarpments is typically 30–80 m, and their size can vary significantly.
- Individual ridges and escarpments are sometimes composed of separate segments that are diagonally aligned.
- When only one diagonal feature is present, it is often more of an escarpment type.
- When several diagonal landforms run in parallel to each other, they are often more of a ridge type.
- Murtoo-related ridges typically have steeper and gentler slopes transverse to the longitudinal axis, and the width of the ridge may vary considerably.
- Occasionally, MREs have a wave-like appearance.
- Locally, MREs display a high degree of parallel conformity. However, contrary to the murtoo landforms, the orientation of MREs can vary within a single murtoo field.
- The direction of MREs often differs from the local ice-flow direction, but is convergent with the direction of subglacial meltwater drainage or/and reflects changes in the underlying terrain topography.
- When appearing in a valley wall or lee side position, the orientation of MREs is often perpendicular to the ice-flow direction.

The more distinct forms of murtoos (TTMs, CTMs and LTMs) and extensive MREs are frequently associated with smaller-scale mounds and ridges, which are here named murtoo-related polymorphous landforms (PMRs; Fig. 3E). Their appearance is complex and difficult to precisely delineate. However, the general characteristics of what are described as PMRs are the following:

- PMRs are irregularly spaced variable-sized (typically 5–100 m in width and length) mounds and ridges that are randomly orientated or orientated in the main direction of close-lying murtoos or MREs.
- When appearing as short ridges, their longer axis is well defined.
- The spacing of PMRs is irregular, even within an individual murtoo field.
- PMRs are commonly found in most murtoo fields.
- PMRs sometimes exhibit murtoo characteristics, but only so weakly developed that it is difficult to classify them as one of the main murtoo types given above.

Morphometry of chevron- and lobate-type murtoos

A total of 200 chevron-type (CTMs) and lobate-type murtoos (LTMs) were measured in the present study. Due to random selection, the spread of the analysed

Table 1. Statistics for the measured chevron-type murtoos (CTMs; $n = 100$), lobate-type murtoos (LTMs; $n = 100$) and triangle-type murtoos (TTMs; $n = 680$) based on Ojala *et al.* (2019a).

	Minimum	1st quartile	Median	Mean	3rd quartile	Maximum
Triangle-type murtoos (TTMs)						
Area (m^2)	90.0	1421.0	2802.5	5458.3	6149.5	73 700.0
Length (m)	9.8	41.5	59.2	74.7	91.9	426.7
Width (m)	16.6	52.1	71.5	85.2	105.7	354.7
Height (m)	0.3	1.9	2.8	3.2	4.1	15.8
Horizontal tip angle γ (°)	24.8	56.9	70.8	71.6	85.4	126.8
Proximal slope α (°)	0.2	2.1	3.7	4.9	6.2	35.9
Distal slope β (°)	1.5	7.0	10.3	11.0	14.6	27.2
Chevron-type murtoos (CTMs)						
Length (m)	30.9	74.2	98.9	112.2	136.7	326.1
Width (m)	32.8	75.3	108.6	119.1	145.1	312.1
Height (m)	1.0	2.1	3.2	3.3	3.8	8.2
Horizontal tip angle γ (°)	37.0	54.8	63.5	63.0	72.0	96.0
Proximal slope α (°)	0.4	1.2	1.7	1.9	2.2	5.8
Ridge proximal slope δ (°)	0.8	2.3	3.1	3.5	4.2	9.4
Distal slope β (°)	1.7	6.5	8.2	8.3	10.1	13.9
Lobate-type murtoos (LTMs)						
Area (m^2)	1801.0	7794.5	16 409.0	24 105.7	25 333.8	166 844.0
Length (m)	36.2	84.7	122.4	132.1	162.4	362.9
Width (m)	60.3	129.7	169.1	191.6	224.0	746.6
Height (m)	1.3	2.7	3.7	4.0	5.2	11.3
Horizontal tip angle γ (°)	43.0	73.8	80.0	81.6	90.0	114.0
Proximal slope α (°)	0.0	1.0	1.6	2.3	2.7	14.0
Distal slope β (°)	4.5	9.0	11.4	12.3	14.5	27.4

landforms is spatially extensive and includes various types of murtoo sites within different ice lobes (Fig. 4).

The range and typical dimensions of LTMs and CTMs are generally similar to TTMs (Ojala *et al.* 2019a; Fig. 5, Table 1). The typical length of LTMs and CTMs in the present data set is 40–240 m (mean 132.2 m) and 40–200 m (mean 112.2 m), respectively. The widths of TTMs and CTMs are very similar (30–200 m), whereas the LTMs are somewhat wider, typically 80–300 m (mean 191.6 m) (Fig. 5B, C). The values of the horizontal tip angle (γ) are within the same range for different murtoo types, although LTMs and CTMs are centred around 60° and 80°, respectively (Fig. 5D). Importantly, the relief of all murtoo types is very similar, commonly <5 m and with a mean of 3.2 m for TTMs, 3.3 m for CTMs and 4.0 m for LTMs (Fig. 5E). The values of the distal slope (β) are also consistent between different murtoo types, although LTMs lack landforms with a slope of >15°, which often appear among TTMs.

In agreement with TTMs, the larger-sized and higher-relief LTMs typically have steeper distal slopes (β) than smaller ones, as indicated by their statistical relationship (Fig. 6A). This relationship does not exist for CTMs. However, all murtoo types show a strong relationship between their length and width, indicating that longer murtoos are also wider. There is also a weak statistical relationship between the width and height for CTMs, but not for TTMs or LTMs (Fig. 6C). The statistical

relationship between distal (β) and proximal (α) slopes is not very strong for any of the murtoo types when applied to the entire data set. However, as illustrated by Fig. 6D, the relationship is moderate for landforms with less steep (<7°) proximal slopes as was already suggested by Ojala *et al.* (2019a). Furthermore, the proximal slopes (α) of TTMs (mean 4.9°) are often significantly steeper than those of LTMs (mean 2.3°), while the slope angle distribution of CTMs spreads at the lower end of TTMs.

Morphometry of murtoo-related ridges and escarpments

Murtoo-related ridges and escarpments (MREs) are typically 100–1000 m long (mean 562.7 m), but can in cases be up to several kilometres long (Fig. 7, Table 2). They are mostly 10–100 m wide (mean 48.6 m), with a strong statistical relationship between their width and length (Fig. 8A). The relief of MREs is mostly <5 m with a mean of 3.5 m, which is very similar to TTMs (Ojala *et al.* 2019a) as well as the LTMs and CTMs presented above (Table 1). A characteristic feature for MREs is that their steeper slopes (ζ) are often 2–10 times steeper than the gentler slopes (ϵ). However, these variables do not have a statistically relevant relationship (Fig. 8C). The slope angles are typically 10–25° for ζ (mean 15.7°) and 0–6° for ϵ (mean 3.4°). Higher-relief landforms have steeper slopes, whereas the height of MREs is only moderately related to the width or length of a landform (Fig. 8B, D).
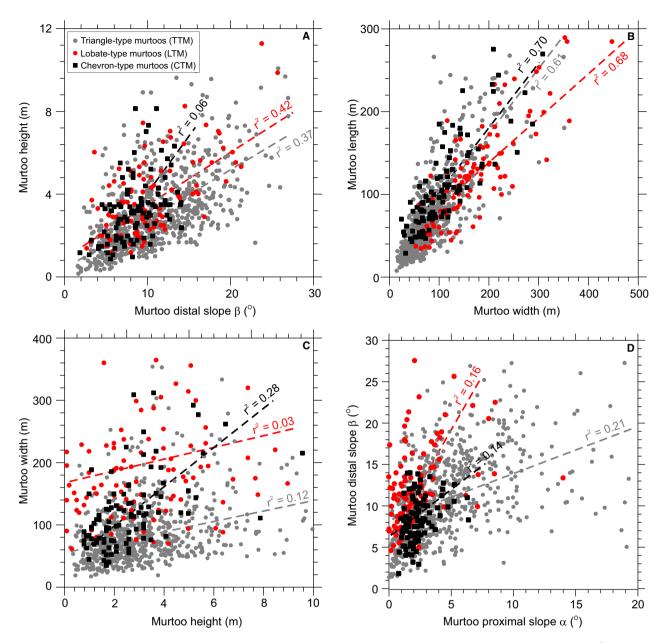
Fig. 6. Statistical relationships between the dimensions and slopes of different murtoo types with linear trend lines and correlations (r²). The data for the triangle-type murtoos (TTMs) are based on Ojala *et al*. (2019a).

Geomorphology and sediment characteristics of the excavated murtoo-related landforms

The airborne LiDAR DEMs of the excavated study sites provide examples of the diversity of murtoo-related landforms that are spatially and morphologically associated with TTMs (Fig. 9; see also Mäkinen *et al.* 2017; Ojala *et al.* 2019a). The four examples described here are typical for each specific site and more generally for the entire FIS area where distinct murtoo fields appear.

In the Kullaa area (Ku in Fig. 4), murtoo-related PMRs occur in association with and partially draping TTMs (Fig. 9A). The shape of these landforms varies from oval mounds to more elongated ridges that are orientated in the direction of latest ice flow, from northwest to southeast. The excavated ridge represents one of the lowest relief landforms in the area and does not show any significant differences in slope angles. In the south/southwest sector of this field, the TTMs and murtoo-related landforms are cut off by fan-shaped hollows, which exhibit more levelled and lower-lying terrain.

At the Kämmäkkä site (Kä in Fig. 4), the murtoo-related PMRs show an oblique morphology that generally appears parallel or transverse to the last ice-flow direction (Fig. 9B). The start and end points of the
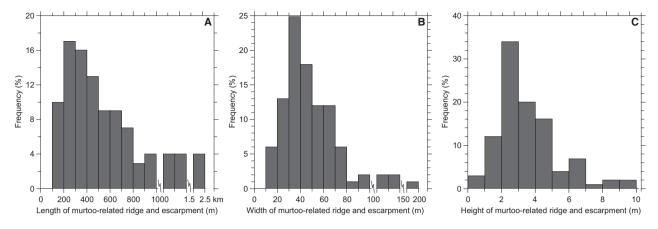
Fig. 7. Variability in the dimensions of the presently studied murtoo-related ridges and escarpments (MREs).

consecutive ridges align, with only small gaps between them. The most prominent ridges lie in the middle of the murtoo field, one of which was excavated in the present study. The sides of these ridges and mounds are often diagonally aligned, although their sizes and reliefs vary considerably. Some of the landforms in this area clearly exhibit a triangular shape, thus being TTMs or CTMs by definition.

The Mikkeli northern and southern study sites are located only about 1 km apart (Mi in Fig. 4). Dominant geomorphological features at the Mikkeli northern site are TTMs orientated up-flow to the latest ice-flow direction with subordinate occurrence of CTMs (Fig. 9C). The excavation presented here was performed across the left-hand limb of a CTM, whereas a cross-section over the nose of a nearby TTM is presented in Mäkinen *et al.* (2019). The orientation of CTM limbs and the areas they enclose are concordant with the other murtoo landforms in the area, implying that they relate to a similar formation process and environment.

In the southern Mikkeli area, located 1 km S-SW from the Mikkeli northern site, murtoo landforms vary from sharp-tipped TTMs to more LTMs in the north and complete or incomplete CTMs in the south (Fig. 9D). An interesting feature in this area is that some of the murtoo-related landforms in the southern part of the area are more of an escarpment type (MRE) than having chevron forms, yet they show an orientation that is consistent with the sides of different murtoo types. In places, the microtopography shows irregular patterns of small hummocks and hollows upon murtoo surfaces.

Sediment characteristics of murtoo-related ridges (MREs, PMRs) and CTMs in trench excavations at the study sites (Fig. 4) are shown in Fig. 10. In general, all the excavated landforms reveal similar main sediment characteristics and overall weakly stratified composition. These include poorly to very poorly sorted massive and matrix-supported to crudely stratified gravel and sandy diamicton, which are interbedded with poorly preserved, mostly laminated and weakly deformed coarse silt to fine (–medium) grained sand beds (Fig. 10B, E). The contacts between diamictons and sandier to gravelly beds are mostly amalgamated and poorly defined. Also, massive looking sand beds mixed with mainly pebble-sized clasts are typical, resembling a 'raisin-cake'-like structure (Fig. 10C). The bed contacts are also mixed or amalgamated. These sediment characteristics are very similar to that of TTMs described by Mäkinen *et al.* (2017, 2019). Also similar to TTMs, clay contents of PMRs and CTMs are low (about 1%), boulders inside these landforms are less than 1 m in diameter, clast roundness is poor (dominantly subangular), and the deposits lack pervasive glaciotectonic deformation (Fig. 10A–D; see also Mäkinen *et al.* 2017, 2019). All murtoo types and murtoo-related landforms are draped by a loose, bouldery and very poorly sorted massive diamicton mantle. It is typical that large boulders or erratics appear on surfaces of murtoos and murtoo-related landforms and their margins often

Table 2. Statistics for the measured murtoo-related ridges and escarpments (MREs; *n* = 100).

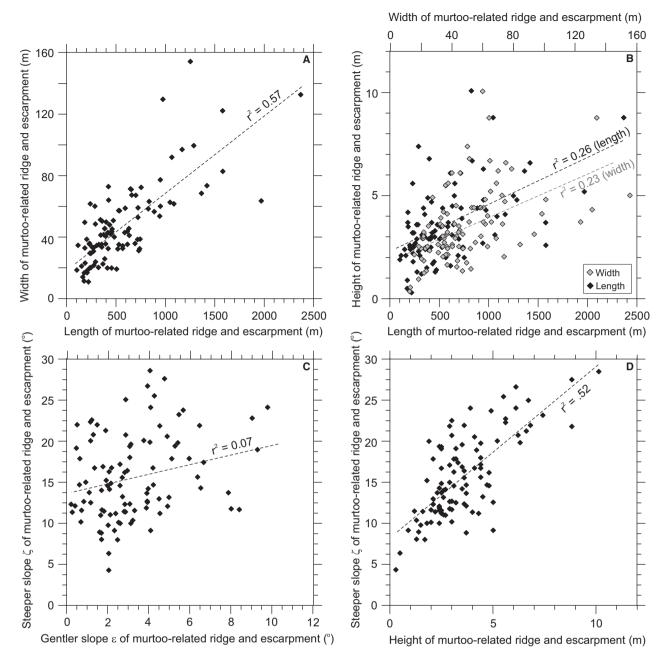|	Minimum	1st quartile	Median	Mean	3rd quartile	Maximum
MREs						
Length (m)	100.1	285.8	436.7	562.7	712.0	2351.5
Width (m)	12.4	33.8	43.0	48.6	60.4	154.2
Height (m)	0.3	2.4	3.1	3.5	4.4	10.1
Steeper slope ζ (°)	4.3	11.7	14.7	15.7	19.5	28.6
More gentle slope ε (°)	0.2	1.8	2.8	3.4	4.3	14.0

Fig. 8. Statistical relationships between the dimensions and slopes of murtoo-related ridges and escarpments (MREs) with linear trend lines and correlations (r^2).

exhibit erosional characteristics with bouldery channels (Mäkinen *et al.* 2017, 2019).

Spatial distribution of murtoos and murtoo-related landforms in Finland

A total of 1154 fields of murtoos and murtoo-related landforms were mapped and recorded in the database in the present study (Fig. 11). Of these, 28.5% were dominated by TTMs, 21.3% by CTMs, 2.8% by LTMs,

37.5% by MREs and 10.1% by PMRs. In most cases (approximately 90–95%), the mapped murtoo fields do not contain only one type of murtoo and/or murtoo-related landforms, but rather there is an number of murtoo types alongside the dominant type even within a limited area. The typical land area of mapped fields of murtoos and murtoo-related landforms is 0.5–1.5 km^2. Within these murtoo fields, there is a significant variation in size of the specific murtoo types (Table 3).
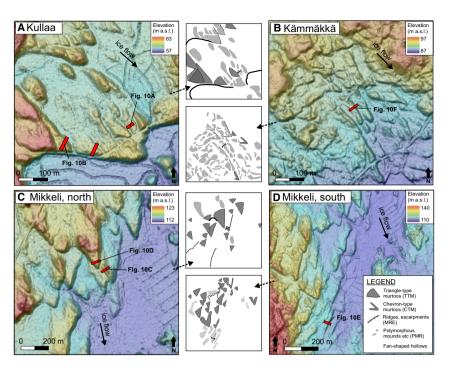
Fig. 9. Hillshaded LiDAR DEM examples of murtoos and murtoo-related ridges and escarpments from excavated sites with mapped morphological interpretations (A = Kullaa; B = Kämmäkkä; C = Mikkeli north; D = Mikkeli south). Black arrows indicate the Late Weichselian ice-flow direction and red bars indicate locations of excavated trenches.

The study by Ojala *et al*. (2019a) had an emphasis on triangle-type murtoos (TTMs; Fig. 1). With the introduction of other types in this study (CTMs, LTMs, MREs and PMRs) we find that murtoos and murtoo-related landforms are much more widespread in Finland than previously presented (Fig. 11). Seen from north to south, scattered MREs are identified in several places in the Inari ice lobe in northern Finland. In line with Ojala *et al*. (2019a), we find no indication of murtoos or murtoo-related landforms within or in the vicinity of the ice-divide zone, where the FIS was cold-based during much of the Late Weichselian (e.g. Kleman & Hättestrand 1999; Boulton *et al*. 2001). Murtoos and murtoo-related landforms are also absent from the Salla ice lobe area (Fig. 11).

We find a pronounced appearance of different murtoo types and murtoo-related types in the Kuusamo ice lobe area, which was not previously recorded by Ojala *et al*. (2019a). This discrepancy is due to TTMs not being the dominating murtoo type but rather MREs being the predominant type with scattered fields of LTMs, CTMs and TTMs. Likewise, the occurrence of murtoos and murtoo-related landforms in the Oulu–North Karelian ice lobe area is clearly more common and widespread than presented in Ojala *et al*. (2019a). In particular, the southern sector of the central part of this ice lobe has an abundance of different types of murtoo fields. The passive-ice areas (e.g. Boulton *et al*. 2001; Putkinen *et al*. 2017) in between the Kuusamo, Oulu–North Karelian

and Finnish Lake District ice lobes are almost completely lacking murtoo landforms (Fig. 11).

Murtoos and murtoo-related landforms are widely distributed in the Finnish Lake District ice lobe area (Fig. 11). As already noted in Ojala *et al*. (2019a), there are two main clusters in the NW and SE parts of the ice lobe. The area in between these clusters is characterized by less extensive fields of CTMs and MREs that appear in distinct corridors (Fig. 11). We have also identified a substantial number of murtoos and murtoo-related landforms dispersed along the boundaries of the NW part of the Näsijärvi–Jyväskylä ice lobe, most of which were not reported in Ojala *et al*. (2019a). Murtoo landforms are, however, absent from the central and SE parts of the Näsijärvi–Jyväskylä ice lobe.

In accordance with Ojala *et al*. (2019a), murtoo fields are common and widespread in the northern part of the Baltic Sea ice lobe area, extending from the western coast of Finland all the way to the Salpausselkä III region. In addition to exceptionally pronounced TTM fields (Mäkinen *et al*. 2017), our data set also shows that there are numerous MRE fields in this area (Fig. 11), again forming distinct corridors in the ice-flow direction. The southern part of the Baltic Sea ice lobe lacks murtoos and murtoo-related landforms. Additionally, scattered murtoo fields and MREs are also evident in the passive-ice triangular area between the Näsijärvi–Jyväskylä, Baltic Sea and Finnish Lake District ice lobes, as well as near the southern coast of Finland.
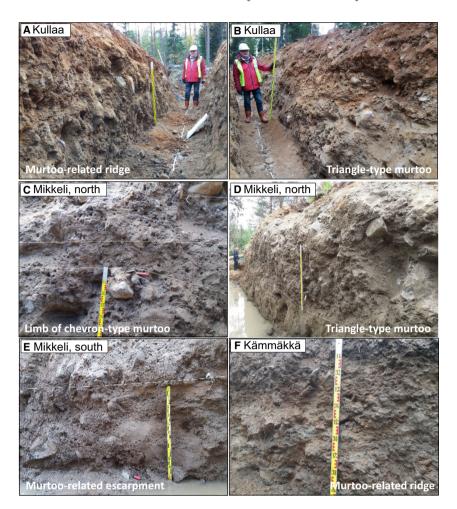
Fig. 10. Photographs showing the subsurface sediments of a murtoo-related ridge (A) and a triangle-type murtoo (B) at the Kullaa site, a limb of a chevron-type murtoo (C) and a triangle-type murtoo (D) at the Mikkeli north site, a murtoo-related escarpment (E) at the Mikkeli south site and a murtoo-related ridge (F) at the Kämmäkkä site. Note that all landforms reveal similar sediment characteristics with crudely stratified gravel and sandy diamicton. All photographs are of walls of excavated trenches (see Figs 4 and 9 for the locations).

Finally, we note that different murtoo types and murtoo-related landforms do not show any clear pattern of spatial distribution (Fig. 11). For example, CTMs and MREs are rather evenly distributed around all ice lobe areas where TTMs also exist (Ojala *et al.* 2019a).

Discussion

Diversity and distribution of murtoos and murtoo-related landforms in Finland

Based on extensive screening of LiDAR DEMs in the FIS area in Finland, we find that the triangular-shaped murtoos (TTMs) with an asymmetric longitudinal profile and apices pointing in the ice-flow direction as described by Mäkinen *et al.* (2017), Peterson *et al.* (2017) and Ojala *et al.* (2019a) are only one diagnostic morphological shape characteristic of murtoo landforms. Our examples (Figs 3, 9, 10) and the statistics of

their dimensions (Figs 5–8) show significant diversity and variability in the shape, relief and size of landforms found in murtoo fields and in association with pure TTMs. Such morphological diversity is common and well established also within other subglacial landforms, such as drumlins (e.g. Clark *et al.* 2009), ribbed moraine (e.g. Möller & Dowling 2018) and polygenetic hummocky moraine (Middleton *et al.* 2020).

The commonalities that link different murtoo types (TTM, CTM and LTM) and murtoo-related landforms (MRE and PMR) are that (i) they all exist in fields or swarms rather than in isolation, (ii) different types occur in the same fields and/or along the same meltwater corridors, (iii) they have similar morphometric characteristics and (iv) they contain similar sediments and sediment architecture. This indicates that these landforms are formed in a common environment, even though many questions remain about the exact subglacial processes that formed them (see Mäkinen *et al.* 2017, 2019).
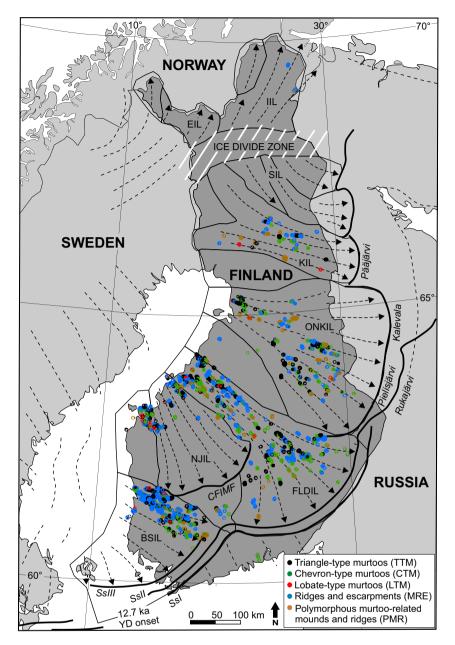
Fig. 11. Distribution of different murtoo types (TTMs, CTMs and LTMs) and murtoo-related landforms (MREs and PMRs) in the Finnish area of the Fennoscandian Ice Sheet. See Fig. 1 for abbreviations of ice lobes and ice-marginal formations.

The spatial distribution of murtoos and murtoo-related landforms in Finland is, as presented here, highly consistent with that of Ojala *et al.* (2019a) for TTMs. The fields of murtoos and murtoo-related landforms (i) are clearly associated with patterns of Late Weichselian and Early Holocene ice lobes in Finland; (ii) mostly appear in areas of the Baltic Sea, Finnish Lake District and Oulu–North Karelian ice lobes and in the onset area of the Näsijärvi–Jyväskylä ice lobe; and (iii) occur in places of rapid ice retreat and in association with significant meltwater flow (Fig. 11) (see also Ahokangas *et al.* 2020). Our results indicate, however, that even though the general pattern of their distribution is similar, the number of fields that contain murtoos and murtoo-related landforms in these areas is significantly higher than proposed by Ojala *et al.* (2019a). This 7–8 times higher occurrence is due to the fact that while Ojala *et al.* (2019a) only included distinct TTMs, the present mapping and analysis expanded murtoo diversity to cover landforms that are closely similar to TTMs (Fig. 3). Another important observation is that different types of murtoo fields are spatially connected and that none of the types presented in Fig. 3 is clustered at an ice-sheet scale.

Table 3. General statistics for the field areas (km^2) of murtoos (TTMs, CTMs and LTMs) and murtoo-related landforms (MREs and PMRs) mapped in this study.

	Minimum	1st quartile	Median	Mean	3rd quartile	Maximum
Triangle-type murtoos (TTMs)	0.01	0.15	0.77	1.53	1.68	14.40
Chevron-type murtoos (CTMs)	0.02	0.31	0.50	1.01	1.15	10.74
Lobate-type murtoos (LTMs)	0.03	0.13	0.31	0.86	1.00	5.74
Murtoo-related ridges and escarpments (MREs)	0.03	0.30	0.70	1.33	1.53	33.72
Murtoo-related polymorphous landforms (PMRs)	0.05	0.31	0.57	1.11	1.36	9.10

The present analysis of murtoos and murtoo-related landforms also supports the idea by Ojala *et al.* (2019a) that they occur in distinct corridors parallel to the regional ice flow and in association with significant meltwater routes (see Ahokangas *et al.* 2020). This pattern is particularly elucidated by the occurrence of elongated fields of murtoo-related ridges and escarpments, which often connect fields of distinct TTMs and CTMs. In fact, only very few and scattered murtoos lie outside these corridors, which is not surprising given the importance of thawed bed conditions and the discharge of subglacial water in their formation (Mäkinen *et al.* 2017; Ojala *et al.* 2019a).

Consistently with TTMs and other murtoo types (Ojala *et al.* 2019a), MREs and PMRs have characteristics that are divergent from other commonly known subglacial landforms. These landforms do not indicate the ice-flow direction in the same way as drumlins, flutings and ribbed moraine tracts in the FIS area (e.g. Punkari 1980; Boulton *et al.* 2001; Lindén *et al.* 2008; Möller & Dowling 2018). Moreover, Peterson *et al.* (2017) and Ojala *et al.* (2019a) demonstrated that murtoo fields cross-cut ribbed moraines, indicating that they were formed at a later stage. The examples of bedform morphology near Harjavalta (Finland) given by Ely *et al.* (2016) are similar in size to murtoos and murtoo-related PMRs, but they do not exhibit triangular-, chevron- or ridge-like appearances, though they are located only a few kilometres NW of a murtoo field mapped in this study. An interesting viewpoint is, however, that different types of landforms appear within a limited area, that were probably formed by somewhat different processes.

Some PMRs are morphologically rather similar to the seismically induced squeeze-up ridges reported by Sutinen & Ojala (2018) and crevasse-squeezed ridges formed closer to the ice front (Evans *et al.* 2020). Larger fields of crevasse-squeezed ridges, however, often exhibit a rhombohedral pattern, like those described in the Svalbard region by Dowdeswell & Ottesen (2016), which is not detected in murtoo fields. Moreover, the PMRs described here appear in murtoo fields that formed further away from the ice margin (see Ojala *et al.* 2019a) and are mostly found in areas lacking glacially induced faults or landslides (e.g. Ojala *et al.* 2019b, c) indicative of palaeoseismicity. An exception to this pattern is the Kemijärvi hummocky moraine field in the Kuusamo ice lobe area, where also murtoos and murtoo-related landforms are present. They have been suggested to be formed in association with Early Weichselian fault instability and subglacial outburst(s) of water and water-saturated sediments (Middleton *et al.* 2020). This might indicate that murtoos can be formed in different subglacial environments, where the distribution and excess of sediment-saturated water plays an essential role.

Geomorphological evidence of subglacial formation

Recent studies have demonstrated significant spatial and morphological variability of subglacial landforms, for example, due to changing basal thermal regimes and the dynamic behaviour of ice sheets (e.g. Mulligan *et al.* 2019; Evans *et al.* 2020). In examining the geomorphic characteristics of murtoos, it is important to recognize that a distinction between murtoo-type 'end members' (Fig. 3) is often difficult as many of them possess overlapping characteristics. Moreover, in places, the dominant murtoo type of a field is difficult to determine, because some murtoo fields may contain up to 100 individual landforms, with approximately an equal number of different murtoo types and/or an abundance of their transition types.

An example of transitions between murtoo types is well established at the Mikkeli sites, where the separation between TTMs or CTMs and murtoo-related escarpments is not straightforward (Fig. 9). However, as described in these examples, the spatial and morphometric relationships of different murtoo types are obvious and the sediment characteristics they display are very similar. As such, they provide evidence that subglacial processes controlling their formation, such as meltwater input, subglacial effective pressure, sediment-concentrated flows, glaciotectonic deformation and postdepositional channel erosion (Mäkinen *et al.* 2019), are interconnected, but can vary in time and space, even within a limited area. It has been argued that seasonal variations in effective pressure alone have a substantial effect on basal sliding and the creep closure of subglacial cavities, causing marked differences in bed strength, bed rheology and sediment distribution (e.g. Lindén *et al.* 2008; Hoffman & Price

Drainage system:	**Linked cavities** Distributed	**Canals/conduits** Semi-distributed	**Tunnel** Channelized

Fig. 12. Cartoon depicting down-ice change in drainage system and related landforms along subglacial meltwater routes where murtoos and murtoo-related landforms exist within the palaeo-ice-stream beds in the Finnish area of the Fennoscandian Ice Sheet. Note that Lewington *et al.* (2020) describe similar meltwater routes, but with more channelized drainage arranged lateral to a central conduit with weakly connected variable pressure axis (VPA) zone that finally connects to eskers. However, their model is typical of non-palaeo-ice-stream beds, whereas palaeo-ice-stream beds likely favour a more distributed (semi-distributed) system.

2014). For example, the morphometric difference between TTMs and sediment-limited CTMs may indicate that their formation was controlled by slightly different processes and subglacial settings, reflecting seasonality and available space in cavities and/or the intensity of sediment-concentrated subglacial flood flow during their formation. An increase in meltwater supply reduces the effective pressure and forces subglacial cavity expansion, thereby increasing discharge in linked-cavity systems (Kamb 1987; Schoof 2010; Davison *et al.* 2019). Furthermore, Mooers (1989) suggested that the formation of sedimentary deposits found in association with tunnel valleys depends on seasonal meltwater delivery reaching the bed via moulins and crevasses, whereas Mäkinen *et al.* (2017, 2019) proposed that murtoos represent a missing element between distributed and channelized drainage systems (Fig. 12).

Mäkinen *et al.* (2019) conclude that TTMs are mainly depositional landforms with erosional heads formed under warm-based ice, where high water pressure and sediment-concentrated subglacial flood flows constantly varied in low conduits or cavities of semi-distributed drainage systems, some 40–60 km behind the ice margin. The demonstrated diversity of murtoo morphology (Fig. 3) supports this observation and clearly indicates that processes controlling subglacial sediment initiation, transport and deposition in this environment are complex both in space and over time. In fact, similarly to drumlins (Clark *et al.* 2009) and ribbed moraine (Lindén *et al.* 2008; Möller & Dowling 2018), the morphological diversity of murtoos is so great that there may not be one single mechanism responsible for their accretionary and erosion patterns (see also Mäkinen *et al.* 2017). The complexity of temperature-dependent rheology of basal ice and its implications for basal hydrological systems were recently discussed by Kasmalkar *et al.* (2019) and McDowell *et al.* (2021), among others. Based

on modelling of subglacial sediment transport, Beaud *et al.* (2018) considered that ice/bed contact conditions must have changed rapidly with a pulse-type behaviour, which is clearly supported by our observations in the murtoo-forming environment in the FIS area. Moreover, a low elongation ratio of TTMs, CTMs and LTMs may indicate slow ice movement and short sediment transport distances, compared to drumlins and flutings, for example (e.g. Clark *et al.* 2009), while concordant relief of all murtoos and murtoo-related landforms (commonly <5 m), may indicate the limited or typical height that a subglacial cavity can grow to in a semi-distributed meltwater system (Fig. 12).

The tendency of murtoos to exhibit diverse morphologies within a limited area also suggests that the subglacial environment in which murtoos were formed constantly evolved and shifted place when experiencing the conditions of a retreating zone that was approaching stagnation during deglaciation (Mäkinen *et al.* 2017; Ojala *et al.* 2019a). Such time-transgressive behaviour is supported by sedimentological evidence from murtoos, which exhibit a shift from subglacial conduit infills to more channelized and finally to route-wide channelized flow conditions in widening subglacial conduits or cavities with sediment-suspension transport (Mäkinen *et al.* 2019; Fig. 12). The distribution of meltwater corridors is important from the ice dynamic perspective as it provides constraints on the magnitude and extent of ice uncoupling via changes in basal water pressure, as was discussed by Lewington *et al.* (2020) in the former Keewatin Ice divide in Canada. Lewington *et al.* (2020) suggest that the scarcity of meltwater routes beneath palaeo-ice streams is due to lower ice-surface slopes and hydraulic gradients, which favour distributed rather than channelized drainage (e.g. Kamb 1987; Bell 2008).

The gradual transitions between murtoos and murtoo-related landforms, which are common in murtoo fields, demonstrate a close relationship in their

formation, which may be associated with constant and smooth seasonal shift in effective pressure and discharge intensity. Lewington *et al.* (2019, 2020) proposed that eskers represent the former existence of central conduits that interacted with a surrounding distributed drainage system when the system was over-pressurized. With murtoos, however, it is possible than instead of central conduits there was a wider braided central murtoo system that widened during the seasonal excess of subglacial meltwater occurring up-ice and prior to the development of a channelized environment (Fig. 12). An example of the development of such a cavity system is murtoo fields that contain both TTMs and more lobate-shaped murtoos (LTMs), as shown by Mäkinen *et al.* (2017) in the Kynäsjärvi murtoo field. In the Kynäsjärvi case, TTMs with a distinct horizontal tip angle (γ) are found in the central part of the field, while LTMs occur in peripheral and higher-lying areas. Depending on the murtoo field geometry, the lower-lying areas in the middle were more prone to water erosion, creating a distinct triangular shape, while rapid clogging of the conduits by mobilized sediments forced water to spread out laterally and away from central area during the highest meltwater delivery. The drawdown of meltwater delivery towards the winter leads to more centralized drainage and an increasingly disarticulated hydrological system, resulting in the collapse of the cavities (see Bartholomaus *et al.* 2011).

Another interesting characteristic is that small ridges and mounds (PMRs) that occur in murtoo fields sometimes exhibit directional patterns that are similar to the nearby TTMs and CTMs, and may thus represent their incomplete forms. PMRs are composed of similar material and sediment architecture (Fig. 10) as in TTMs, which indicates that the environment and formation processes resemble those described by Mäkinen *et al.* (2019). However, based on their shape, their formation may have been terminated because of the filling-in or closure of subglacial cavities, a lack of sediment-concentrated flows, or rerouting of meltwater due to changing pressure conditions. The morphometric diversity of these landforms probably indicates rapid variations in the configuration of subglacial hydrology at different spatial and temporal scales, as well as a complicated relationship between water (and sediment) and motion at the glacier bed (e.g. Bartholomaus *et al.* 2011; Hooke 2019). Studies on modern glaciers have revealed that glacier hydrology and its connection to basal motion is never steady and evolves between drainage in linked cavities or till sheets, efficient channelized flow and high discharge conduits and subglacial groundwater flow (Mair *et al.* 2001; Bartholomaus *et al.* 2011).

The morphometric difference between murtoo types (TTM, CTM and LTM) and MREs, and erosional characteristics, demonstrate the importance of subglacial drainage in their formation along these routes.

MREs in murtoo fields could actually represent pathways that guided hydrological routing along which subglacial meltwater was evacuated towards the R-channels (Röthlisberger 1972; Boulton & Hindmarsh 1987), whereas murtoos represent sediment-concentrated flows and progressive sediment creep in a slightly earlier stage (Fig. 12). Although we don't rule out erosion in shaping TTMs and CTMs in the final stage of their formation, the erosional characteristics of long and continuous ridges and escarpments (MREs) are obvious with their direction often differing from the local ice flow and converging with topography-driven subglacial drainage. This split into more depositional forms (TTMs, CTMs and LTMs) and erosional forms (MREs) is also supported by the sedimentological observations of Mäkinen *et al.* (2019), who claimed that in the last stage of murtoo-forming corridors, subglacial meltwater flows became more channelized and contributed to the final shape of the murtoo margins and narrow passages between adjacent murtoo fields (Fig. 12). In many cases, these corridors with extensive MREs terminate at distinct depressions that have been regarded as subglacial lakes, or at places where eskers begin (Mäkinen *et al.* 2017). The occurrence of lateral channels within murtoo fields and large boulders and irregular ridges and hollows on top of murtoo surfaces indicate the role of water erosion in the final stage of their formation, thus supporting the sedimentological observations by Mäkinen *et al.* (2017, 2019). This suggests that the formation of murtoo-forming drainage corridors took place during different stages in the course of deglaciation and before esker deposition closer to the ice margin, even though Mäkinen *et al.* (2017) demonstrated that not all murtoo fields are associated with distinct eskers.

The distribution of murtoos and murtoo-related landforms has broad implications for the spatial and temporal variations of subglacial hydrology and the intricate regional ice-sheet dynamics. Given the essential role of subglacial drainage in the shaping of glacial landscapes and redistribution of large volumes of sediments in the Finnish area of the FIS, future studies should focus on ice-lobe and sub-lobe scale understanding of the various forms of water evacuation along these routes, which probably operated time-transgressively and produced different types of landforms at the transition from a distributed to channelized environment.

Conclusions

This study demonstrates that the morphometric diversity of murtoos and murtoo-related landforms in the Fennoscandian Ice Sheet area is larger than previously described. Detailed LiDAR-based mapping and analysis of murtoo fields show that five primary types are common and widespread in Finland: (i) triangle-type murtoos (TTMs), (ii) chevron-type murtoos (CTMs),

(iii) lobate-type murtoos (LTMs), (iv) murtoo-related ridges and escarpments (MREs), and (v) other murtoo-related polymorphous landforms (PMRs). Different types of murtoos and murtoo-related landforms are spatially and geomorphologically related, as they typically appear in the same murtoo fields. The site-specific examples given in this study also show that different types of murtoos and murtoo-related landforms share a similar composition and architecture of sediments, which indicates that their formative processes and environment are largely similar. They are all products of subglacial deposition in association with significant subglacial meltwater flow and their diversity indicates the complexity of spatially and temporally shifting ice-sheet basal thermal regimes and its implications for basal hydrology. Our results have broad implications for studies on ice-sheet dynamics and emphasize the essential role of subglacial meltwater in the shaping of glacial landscapes and the redistribution of large volumes of sediments during deglaciation.

References

Ahokangas, E., Mäkinen, J., Ojala, A. E. K., Kajuutti, K. & Palmu, J.-P. 2020: Murtoos and subglacial meltwater routes are significant geomorphological features in the trunk area of the Finnish Lake District Ice Lobe. *NGF Abstracts and Proceedings no 1, 2020*. The 34th Nordic Geological Winter Meeting, 8-10.1.2020, Oslo, Norway.

Alley, R. B., Marotzke, J., Nordhaus, W. D., Overpeck, J. T., Peteet, D. M., Pielke, R. A. Jr, Pierrehumbert, R. T., Rhines, P. B., Stocker, T. F., Talley, L. D. & Wallace, J. M. 2003: Abrupt climate change. *Science* 299, 2005–2010.

Andrews, L. C., Catania, G. A., Hoffman, M. J., Gulley, J., Lüthi, M. P., Ryser, C., Hawley, R. L. & Neumann, T. A. 2014: Direct observations of evolving subglacial drainage beneath the Greenland ice sheet. *Nature* 514, 80–83.

Bartholomaus, T. C., Anderson, R. S. & Anderson, S. P. 2011: Growth and collapse of the distributed subglacial hydrologic system of Kennicott Glacier, Alaska, USA, and its effects on basal motion. *Journal of Glaciology* 57, 985–1002.

Beaud, F., Flowers, G. & Venditti, J. G. 2018: Modeling sediment transport in ice-walled subglacial channels and its implications for esker formation and proglacial sediment yields. *Journal of Geophysical Research: Earth Surface* 123, 3206–3227.

Bell, R. E. 2008: The role of subglacial water in ice-sheet mass balance. *Nature Geoscience* 1, 297–304.

Bell, R., Studinger, M., Shuman, C. A., Fahnestock, M. A. & Joughin, I. 2007: Large subglacial lakes in East Antarctica at the onset of fast-flowing ice streams. *Nature* 445, 904–907.

Benn, D. I. & Evans, D. J. A. 1998: *Glaciers and Glaciation.* 734 pp. Arnold, London.

Boulton, G. & Hindmarsh, R. 1987: Sediment deformation beneath glaciers: rheology and geological consequences. *Journal of Geophysical Research* 92, 9059–9082.

Boulton, G. S., Dongelmans, P., Punkari, M. & Broadgate, M. 2001: Palaeoglaciology of an ice sheet through a glacial cycle: the European ice sheet through the Weichselian. *Quaternary Science Reviews* 20, 591–625.

Bowling, J. S., Livingstone, S. J., Sole, A. J. & Chu, W. 2019: Distribution and dynamics of Greenland subglacial lakes. *Nature Communications* 10, 2810, https://doi.org/10.1038/s41467-019-10821-w.

Clark, C. D., Hughes, A. L., Greenwood, S. L., Spagnolo, M. & Ng, F. S. 2009: Size and shape characteristics of drumlins, derived from a large sample, and associated scaling laws. *Quaternary Science Reviews* 28, 677–692.

Davison, B. J., Sole, A. J., Livingstone, S. J., Cowton, T. R. & Nienow, P. W. 2019: The influence of hydrology on the dynamics of land-terminating sectors of the Greenland Ice Sheet. *Frontiers in Earth Sciences* 7, 10, https://doi.org/10.3389/feart.2019.00010.

Donner, J. 1995: *The Quaternary History of Scandinavia.* 200 pp. Cambridge University Press, Cambridge.

Dow, C. F., Kulessa, B., Rutt, I. C., Tsai, V. C., Pimentel, S., Doyle, S. H., van As, D., Lindbäck, K., Pettersson, R., Jones, G. A. & Hubbard, A. 2015: Modeling of subglacial hydrological development following rapid supraglacial lake drainage. *Journal of Geophysical Research: Earth Surface* 120, 1127–1147.

Dowdeswell, J. A. & Ottesen, D. 2016: Submarine landform assemblage for Svalbard surge-type tidewater glaciers. *In* Dowdeswell, J. A., Canals, M., Jakobsson, M., Todd, B. J., Dowdeswell, E. K. & Hogan, K. A. (eds.): *Atlas of Submarine Glacial Landforms: Modern, Quaternary and Ancient*, 151–154. Geological Society, London, Memoirs 46.

Ely, J. C., Clark, C. D., Spagnolo, M., Stokes, C. R., Greenwood, S. L., Hughes, A. L. C., Dunlop, P. & Hess, D. 2016: Do subglacial bedforms comprise a size and shape continuum? *Geomorphology* 257, 108–119.

Evans, D. J. A., Atkinson, N. & Phillips, E. 2020: Glacial geomorphology of the Neutral Hills Uplands, southeast Alberta, Canada: the process-form imprints of dynamic ice streams and surging ice lobes. *Geomorphology* 350, 106910, https://doi.org/10.1016/j.geomorph.2019.106910.

Flowers, G. E. 2015: Modelling water flow under glaciers and ice sheets. *Proceedings of the Royal Society A: Mathematical, Physical and Engineering Sciences* 471, 20140907, https://doi.org/10.1098/rspa.2014.0907.

Greenwood, S. L., Clason, C. C., Nyberg, J., Jakobsson, M. & Holmlund, P. 2017: The Bothnian Sea ice stream: early Holocene retreat dynamics of the south-central Fennoscandian Ice Sheet. *Boreas* 46, 346–362.

Hermanowski, P. & Piotrowski, J. A. 2019: Groundwater flow under a paleo-ice stream of the Scandinavian Ice Sheet and its implications for the formation of Stargard drumlin field, NW Poland. *Journal of Geophysical Research: Earth Surface* 124, 1720–1741.

Hoffman, M. J. & Price, S. 2014: Feedbacks between coupled subglacial hydrology and glacier dynamics. *Journal of Geophysical Research – Earth Surface* 119, 414–436.

Hooke, R. L. B. 2019: *Principles of Glacier Mechanics.* 618 pp. Cambridge University Press, Cambridge.

Hughes, A. L. C., Gyllencreutz, R., Lohne, Ø. S., Mangerud, J. & Svendsen, J. I. 2015: The last Eurasian ice sheets – a chronological database and time-slice reconstruction, DATED-1. *Boreas* 45, 1–45.

Hughes, P. D., Gibbard, P. L. & Ehlers, J. 2020: The "missing glaciations" of the Middle Pleistocene. *Quaternary Research* 96, 161–183.

Jenness, J. 2013: *DEM surface tools. Jenness enterprises.* Available at http://www.jennessent.com/arcgis/surface_area.htm.

Kamb, B. 1987: Glacier surge mechanism based on linked cavity configuration of the basal water conduit system. *Journal of Geophysical Research – Solid Earth* 92, 9083–9100.

Kasmalkar, I., Mantelli, E. & Suckale, J. 2019: Spatial heterogeneity in subglacial drainage driven by till erosion. *Proceedings of The Royal Society A Mathematical Physical and Engineering Sciences 475*, 20190259. https://doi.org/10.1098/rspa.2019.0259.

Kleman, J. & Hättestrand, C. 1999: Frozen-bed Fennoscandian and Laurentide ice sheets during the Last Glacial Maximum. *Nature 402*, 63–66.

Kleman, J., Hättestrand, C., Borgström, I. & Stroeven, A. 1997: Fennoscandian palaeoglaciology reconstructed using a glacial geological inversion model. *Journal of Glaciology 43*, 283–299.

Kurimo, H. 1980: Depositional deglaciation forms as indicators of different glaciomarginal environments. *Boreas 9*, 179–191.

Lehtinen, M., Nurmi, P. & Rämö, T. 2005: *Precambrian Geology of Finland*. 736 pp. Elsevier, Amsterdam.

Lesemann, J.-E., Piotrowski, J. A. & Wysota, W. 2014: Genesis of the "glacial curvilineation" landscape by meltwater processes under the former Scandinavian Ice Sheet, Poland. *Sedimentary Geology 312*, 1–18.

Lewington, E. L., Livingstone, S. J., Clark, C. D., Sole, A. J. & Storrar, R. D. 2020: A model for interaction between conduits and surrounding hydraulically connected distributed drainage based on geomorphological evidence from Keewatin, Canada. *The Cryosphere 14*, 2949–2976.

Lewington, E. L. M., Livingstone, S. J., Sole, A. J., Clark, C. D. & Ng, F. S. L. 2019: An automated method for mapping geomorphological expressions of former subglacial meltwater pathways (hummock corridors) from high resolution digital elevation data. *Geomorphology 339*, 70–86.

Lindén, M., Möller, P. & Adrielsson, L. 2008: Ribbed moraine formed by subglacial folding, thrust stacking and lee-side cavity infill. *Boreas 37*, 102–131.

Lundqvist, J. & Saarnisto, M. 1995: Summary of project IGCP-253. *Quaternary International 28*, 9–18.

Mair, D., Nienow, P., Willis, I. & Sharp, M. 2001: Spatial patterns of glacier motion during a high-velocity event: Haut Glacier d'Arolla, Switzerland. *Journal of Glaciology 47*, 9–20.

Mäkinen, J., Kajuutti, K., Ojala, A., Ahokangas, E. & Palmu, J.-P. 2019: Sedimentary characteristics of Finnish MURTOOs - triangular-shaped subglacial landforms produced during rapid retreat of continental ice sheets. *Advances in Glacier Hydrology III Posters, C13C-1309*. AGU Fall Meeting San Francisco CA, 9–13 December 2019.

Mäkinen, J., Kajuutti, K., Palmu, J.-P., Ojala, A. & Ahokangas, E. 2017: Triangular-shaped landforms reveal subglacial drainage routes in SW Finland. *Quaternary Science Reviews 164*, 37–53.

McDowell, I. E., Humphrey, N. F., Harper, J. T. & Meierbachtol, T. W. 2021: The cooling signature of basal crevasses in a hard-bedded region of the Greenland Ice Sheet. *The Cryosphere Discussions 15*, 897–907.

Middleton, M., Nevalainen, P., Hyvönen, E., Heikkonen, J. & Sutinen, R. 2020: Pattern recognition of LiDAR data and sediment anisotropy advocate a polygenetic subglacial mass-flow origin for the Kemijärvi hummocky moraine field in northern Finland. *Geomorphology 362*, 107212, https://doi.org/10.1016/j.geomorph.2020.107212.

Möller, P. & Dowling, T. P. F. 2018: Equifinality in glacial geomorphology: instability theory examined via ribbed moraine and drumlins in Sweden. *GFF 140*, 106–135.

Mooers, H. 1989: On the formation of tunnel valleys of the Superior Lobe, Central Minnesota. *Quaternary Research 32*, 24–35.

Mulligan, R. P. M., Eyles, C. H. & Marich, A. S. 2019: Subglacial and ice-marginal landforms in south-central Ontario: implications for ice sheet reconfiguration during deglaciation. *Boreas 48*, 635–657.

Ojala, A. E. K. 2016: Appearance of De Geer moraines in southern and western Finland – implications for reconstructing glacier retreat dynamics. *Geomorphology 255*, 16–25.

Ojala, A. E. K., Mattila, J., Markovaara-Koivisto, M., Ruskeeniemi, T., Palmu, J.-P. & Sutinen, R. 2019b: Distribution and morphology of landslides in northern Finland – analysis of postglacial seismic activity. *Geomorphology 326*, 190–201.

Ojala, A. E. K., Mattila, J., Ruskeeniemi, T., Markovaara-Koivisto, M., Palmu, J.-P., Nordbäck, N., Lindberg, A., Aaltonen, I., Savunen, J. & Sutinen, R. 2019c: Postglacial faults in Finland – a review of PGSdyn-project results. *POSIVA, Report 2019-1*, 118 pp.

Ojala, A. E. K., Peterson, G., Mäkinen, J., Johnson, M., Kajuutti, K., Ahokangas, E., Palmu, J.-P. & Öhrling, C. 2019a: Ice sheet scale distribution of unique triangular-shaped hummocks (murtoos) – a subglacial landform produced during rapid retreat of the Scandinavian Ice Sheet. *Annals of Glaciology 60*, 115–126.

Palmu, J.-P., Ojala, A. E. K., Ruskeeniemi, T., Sutinen, R. & Mattila, J. 2015: LiDAR DEM detection and classification of postglacial faults and seismically-induced landforms in Finland: a paleoseismic database. *GFF 137*, 344–352.

Peterson, G. & Johnson, M. D. 2018: Hummock corridors in the south-central sector of the Fennoscandian ice sheet, morphometry and pattern. *Earth Surface Processes and Landforms 43*, 919–929.

Peterson, G., Johnson, M. & Smith, C. 2017: Glacial geomorphology of the south Swedish uplands–focus on the spatial distribution of hummock tracts. *Journal of Maps 13*, 534–544.

Punkari, M. 1980: The ice lobes of the Scandinavian ice sheet during the deglaciation in Finland. *Boreas 9*, 307–310.

Putkinen, N., Eyles, N., Putkinen, S., Ojala, A. E. K., Palmu, J.-P., Sarala, P., Väänänen, T., Räisänen, J., Saarelainen, J., Ahtonen, N., Rönty, H., Kiiskinen, A., Rauhaniemi, T. & Tervo, T. 2017: High-resolution LiDAR mapping of ice stream lobes in Finland. *Bulletin of the Geological Society of Finland 89*, 64–81.

Rada, C. & Schoof, C. 2018: Channelized, distributed, and disconnected: subglacial drainage under a valley glacier in the Yukon. *The Cryosphere 12*, 2609–2636.

Rainio, H. 1996: *Late Weichselian End Moraines and Deglaciation in Eastern and Central Finland*. 73 pp. Geological Survey of Finland, Espoo.

Rainio, H., Saarnisto, M. & Ekman, I. 1995: Younger Dryas end moraines in Finland and NW Russia. *Quaternary International 28*, 179–192.

Remy, F. & Legresy, B. 2004: Subglacial hydrological networks in Antarctica and their impact on ice flow. *Annals of Glaciology 39*, 67–72.

Röthlisberger, H. 1972: Water pressure in intra- and subglacial channels. *Journal of Glaciology 11*, 177–203.

Sarala, P. 2006: Ribbed moraine stratigraphy and formation in southern Finnish Lapland. *Journal of Quaternary Science 21*, 387–398.

Schoof, C. 2010: Ice sheet acceleration driven by melt supply variability. *Nature 468*, 803–806.

Shackleton, C., Patton, R., Hubbard, A., Winsborrow, M., Kingslake, J., Esteves, M., Andreassen, K. & Greenwood, S. L. 2018: Subglacial water storage and drainage beneath the Fennoscandian and Barents Sea ice sheets. *Quaternary Science Reviews 201*, 13–28.

Shaw, J., Kvill, D. & Rains, B. 1989: Drumlins and catastrophic subglacial floods. *Sedimentary Geology 62*, 177–202.

Shaw, J., Pugin, A. & Young, R. R. 2008: A meltwater origin for Antarctic shelf bedforms with special attention to megalineations. *Geomorphology 102*, 364–375.

Shreve, R. L. 1972: Movement of water in glaciers. *Journal of Glaciology 11*, 205–214.

Siegert, M. J., Kulessa, B., Bougamont, M., Christoffersen, P., Key, K., Andersen, K. R., Booth, A. D. & Smith, A. M. 2017: Antarctic subglacial groundwater: a concept paper on its measurement and potential influence on ice flow. *Geological Society, London, Special Publications 461*, 197–213.

Sutinen, R. & Ojala, A. E. K. 2018: Paleoseismic deformations in central Finnish Lapland. *PATA days 2018, 9th International INQUA Meeting on Paleoseismology, Active Tectonics and Archeoseismology, 24-28.7.2018, Thessaloniki, Greece.*